Hyperstratification following glacial overturning events in the northern Arabian Sea

Gert-Jan Reichart,[1,2] Henk Brinkhuis,[3] Frank Huiskamp,[4] and Willem Jan Zachariasse[4]

Received 6 August 2003; revised 29 October 2003; accepted 6 January 2004; published 7 May 2004.

[1] Correlations between Arabian Sea organic carbon and GISP2 $\delta^{18}O$ records indicate a pronounced oxygen minimum zone (OMZ) during interstadials, whereas well-oxygenated conditions prevailed during stadials. Local deep winter mixing ventilated intermediate water during the coldest stadials, corresponding to North Atlantic Heinrich events. Here we show that in the Arabian Sea periods of climatic warming following Heinrich events H6–H4 and the Younger Dryas (YD) are characterized by dominant *Polysphaeridium zoharyi* (dinoflagellate) cysts. The finding of assemblages dominated by *P. zoharyi* in the open ocean is unusual because today similar assemblages are restricted to lagoonal settings. It is postulated that the highly saline mixed layer and the strong density gradient which characterized Arabian Sea hydrography after H6–H4 and the YD simulated a shallow seafloor, thereby enabling germination of cysts prior to sinking. The strong density gradient following cold stadials should have facilitated the rapid reestablishment of a pronounced OMZ during interstadials. *INDEX TERMS:* 1050 Geochemistry: Marine geochemistry (4835, 4850); 3030 Marine Geology and Geophysics: Micropaleontology; 4267 Oceanography: General: Paleoceanography; *KEYWORDS:* Arabian Sea, dinoflagelates cysts, oxygen minimum zone

Citation: Reichart, G.-J., H. Brinkhuis, F. Huiskamp, and W. J. Zachariasse (2004), Hyperstratification following glacial overturning events in the northern Arabian Sea, *Paleoceanography*, *19*, PA2013, doi:10.1029/2003PA000900.

1. Introduction

[2] The northern Arabian Sea is presently characterized by one of the largest bodies of oxygen-deficient waters on Earth [*Wyrtki*, 1971]. The fact that the Arabian Sea is landlocked to the north strongly influences intermediate water circulation. Relatively high sea-surface temperatures (SSTs) prevent overturning and water at intermediate depth is consequently ventilated by water formed in the southern Indian Ocean subtropical gyre. At the time this water reaches the Arabian Sea it is poor in oxygen [*Olson et al.*, 1993; *You and Tomczak*, 1993]. This condition, in combination with the high sea-surface productivity due to summer monsoon-driven upwelling, results in a pronounced oxygen minimum between 200 and 1200 m with lowest oxygen concentrations in the northeastern part of the basin [*Swallow*, 1984; *You and Tomczak*, 1993]. This intense oxygen minimum zone (OMZ) drives large-scale denitrification within the water column [*Wyrtki*, 1973; *Naqvi*, 1987] and affects the sedimentary environment where it intersects the seafloor topography [*Von Stackelberg*, 1972; *Jannink et al.*, 1998; *van der Weijden et al.*, 1999].

[3] Changes in surface water productivity and local overturning related to intensified and cold winter monsoonal winds have affected the intensity of the OMZ over time. Short and abrupt changes in OMZ intensity have been synchronized with changes in $\delta^{18}O$ of Greenland ice using wiggle matching [*Reichart et al.*, 1998; *Schulz et al.*, 1998; *Altabet et al.*, 2002; *Reichart et al.*, 2002a]. Cold/warm phases over Greenland correspond to oxygen-rich/oxygen-depleted conditions in the northern Arabian Sea [*Reichart et al.*, 1998; *Schulz et al.*, 1998; *Altabet et al.*, 2002]. The coldest stadials, corresponding to the North Atlantic Heinrich Events, are characterized by deep winter mixing [*Reichart et al.*, 1998; *Reichart et al.*, 2002b], thereby ventilating the OMZ. In contrast, the interstadials following these Heinrich events are accompanied by high summer monsoon driven productivity resulting in a rapid re-establishment of the OMZ. Changes in OMZ intensity in the northern Arabian Sea may have more than regional significance as they may have contributed to glacial variability in atmospheric CO_2 through modification of nutrient availability by denitrification [*Altabet et al.*, 1995, 2002]. Here we report on hydrographic conditions in the Northern Arabian Sea immediately following extreme stadials, combining multidisciplinary datasets with an analysis of the remains of typical surface water dwelling organisms, dinoflagellates.

2. Materials and Methods

[4] Northern Arabian Sea sediment core NIOP478 (24°12.′7 N, 065°39.′7 E, in 565 m water depth; Figure 1) was collected from a location within the OMZ on the Pakistan Margin during the Netherlands Indian Ocean Program (1992–1993) and measures 14.5 m. Sediments consist of dark-greenish to light-greenish/gray hemipelagic muds showing multiple laminated intervals. No turbidites were observed. Sample spacing for this study is 5 cm, corresponding to an average resolution of about 250 yr (see

[1]Alfred Wegener Institut for Polar and Marine Research, Bremerhaven, Germany.
[2]Also at Faculty of Earth Sciences, Utrecht University, Utrecht, Netherlands.
[3]Laboratory of Palaeobotany and Palynology, Utrecht University, Utrecht, Netherlands.
[4]Faculty of Earth Sciences, Utrecht University, Utrecht, Netherlands.

0883-8305/04/2003PA000900$12.00

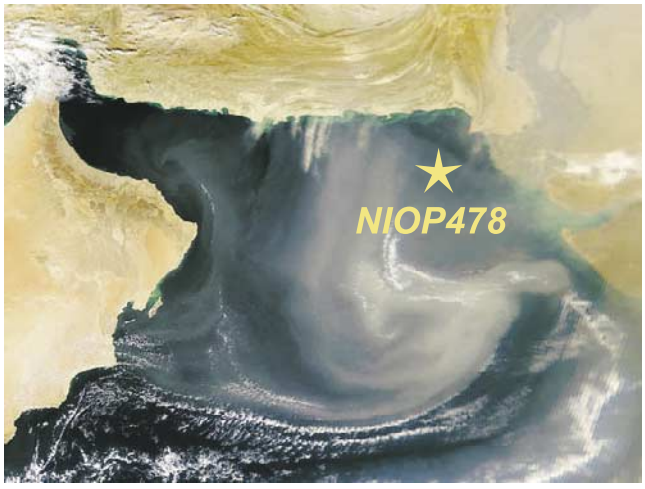

Figure 1. SeaWiFS image showing a massive dust storm in Iran and Pakistan blowing out into the Arabian Sea. Star indicates location of station NIOP478 on the continental margin. (Satellite image provided by the SeaWiFS Project, NASA/Goddard Space Flight Center, and ORBIMAGE. Image date is 12 December 1999.)

below). The chronology for NIOP478 is based on oxygen isotopes and ^{14}C-dates [*Reichart et al.*, 1998, 2002a]. The uppermost part of the sediment succession (corresponding to the last 6000 years) is missing (Figure 2).

[5] For palynological studies, 80 samples were oven dried for 24 hours at 60°C, after which on average 1 gram of sediment was carefully weighed and treated with 10% HCl in order to remove carbonates. Upon addition of demineralized water the samples were left for 24 hours. The samples were then decanted and, in order to remove silicates, shaken for 2 hours at approximately 250 rpm with 38% HF. Demineralized water was again added and samples were allowed to sit for another 24 hours before being decanted and sieved 3 times with a Stork Veco Precision Sieve (Mesh 850, Hole 10). The remaining material was put in micro test tubes (Eppendorf) in 0.5 mL of demineralized water. Slides were made using 1/20 of the material. Entire slides were counted with a minimum of 200 palynomorphs per sample. Nomenclature applied in this study is based on that cited in the work of *Williams et al.* [1998].

[6] Porosity of the sediment was calculated for all samples from weight loss upon freeze-drying fixed volume samples. Organic carbon was measured every other sample using a CNS analyzer (Fisons NA 1500), after prior removal of carbonate, with a relative precision better than 3% [*Reichart et al.*, 1998]. The sediment porosity of NIOP478 shows a good correlation with organic carbon content (Figure 2b). The upper (Holocene) section shows a somewhat better but different relationship between C_{org} and porosity as compared to the older (glacial) section. The two equations relating organic matter and porosity are $C_{org} = e^{3.906*\ln(\text{porosity})-14.1974}$ for the Holocene and $C_{org} = e^{3.774*\ln(\text{porosity})-13.0122}$ for the Glacial. The reason for the observed time dependency is most likely related to a change in biogenic versus abiogenic particles. Biogenic particles have a more "open" structure, whereas the abiogenic particles are massive. Since the time resolution of the porosity data is twice that of the C_{org} data we used the porosity data to predict C_{org} proxy values for all samples.

[7] Sr and Ca concentrations, occurrences of *Globorotalia truncatulinoides* and *Globorotalia crassaformis*, and pteropod numbers are from *Reichart et al.* [1998]. Sea-surface salinities (SSS) calculated by combining the alkenone-based SST reconstruction with planktonic and benthic foraminiferal oxygen isotope data are from *Reichart et al.* [2002b]. Element concentrations for Ti and Al were measured by inductively coupled plasma (ICP) atomic emission spectrometry (AES) (PerkinElmer Optima 3000). For this purpose a part of the sample was dried at 60°C for 4 days, thoroughly ground in an agate mortar prior to $HClO_4$, HNO_3, and HF acid digestion. The final residue was taken up in 1 M HCl. Comparison with international (SO-1) and in-house (MM-91) standards and the analyses of duplicate samples revealed that relative standard deviations, analytical precision, and accuracy were better than 3%.

3. Results

[8] *Reichart et al.* [1998, 2002a] and *Schulz et al.* [1998] showed a high degree of similarity between northern Arabian Sea C_{org} curves and the δ^{18}O records of GISP2 and GRIP [*Dansgaard et al.*, 1993; *Grootes et al.*, 1993]. The pattern of predicted C_{org} values of NIOP478 mimics the Greenland oxygen isotope record, even beyond the Dansgaard-Oeschger variability (Figure 2a). This confirms that C_{org} changes in the northern Arabian Sea and δ^{18}O changes in the GISP2 ice core are in phase and synchronous [*Schulz et al.*, 2002].

[9] Organic carbon values, Sr/Ca ratios, and pteropod numbers all show rapid changes, which to varying degrees follow the δ^{18}O changes in the GISP2/GRIP ice cores (Figure 2a). Interstadials correlate with high organic carbon values, low Sr/Ca ratios and the absence of pteropod tests (Figure 2). Stadials show an inverse relationship; the coldest stadials (corresponding to Heinrich events) are characterized by appearances of the deep-dwelling planktonic foraminifera *G. truncatulinoides* and *G. crassaformis* (Figure 2), by maximum pteropod numbers (up to 1200 specimen per gram), and by highest Sr/Ca values. Some of the less cold stadials are characterized by less abundant pteropods and slightly raised Sr/Ca values. While Heinrich events H6, H4 and H1 are clearly characterized by the occurrence of deep dwelling foraminifera, both H3 and H2 lack these species. The Ti/Al ratio shows a distinct minimum during the deglaciation and several smaller scale maxima in the glacial section (Figure 3). These glacial Ti/Al maxima tend to coincide with high pteropod numbers.

[10] Figure 2c shows that Sr and Ca values are closely related, but their ratio changes abruptly when the Ca concentration reaches values over ~12.5%. Whereas at low Ca concentrations Sr values increase by about 70 ppm for every percent Ca, this ratio more than quadruples at concentrations over ~12.5% Ca, with Sr values increasing by 370 ppm with each extra percent Ca (Figure 2c). Such a distinct change in slope indicates that Sr and Ca are present in at least two separate phases with different Sr/Ca ratios.

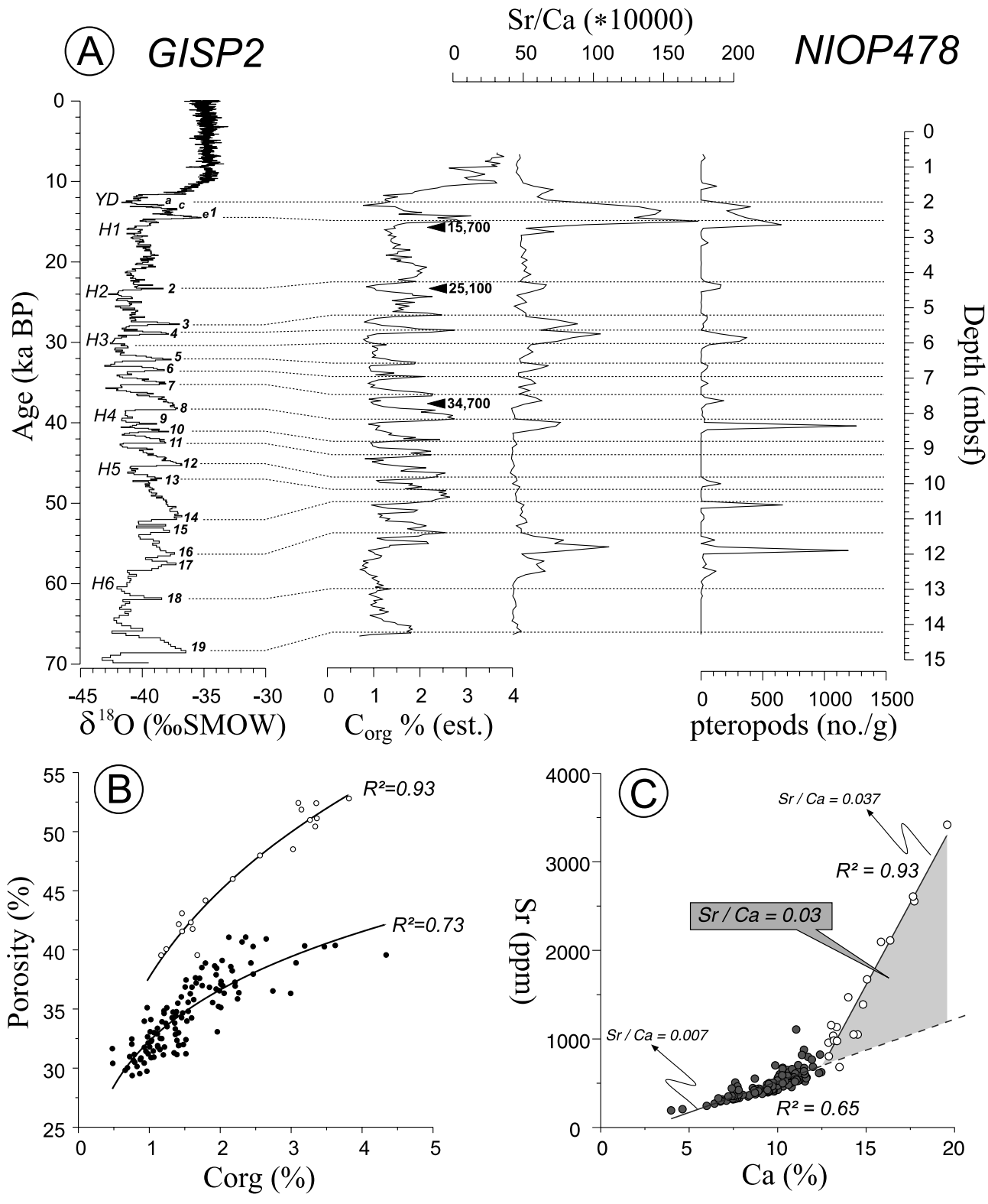

Figure 2. (a) Correlation between the oxygen isotope record of the GISP2 Greenland ice core and the predicted organic carbon record of NIOP478. Numbers 1–19 refer to interstadials in ice core. Also indicated are Sr/Ca and pteropod counts [*Reichart et al.*, 2002b]. (b) Correlation between measured C_{org} content and sediment porosity. The two indicated correlations are used for predicting the organic carbon as plotted in Figure 2a. (c) Relation between the Ca and Sr contents of the bulk sediment. Gray area indicates the Sr/Ca relationship of the high Sr component.

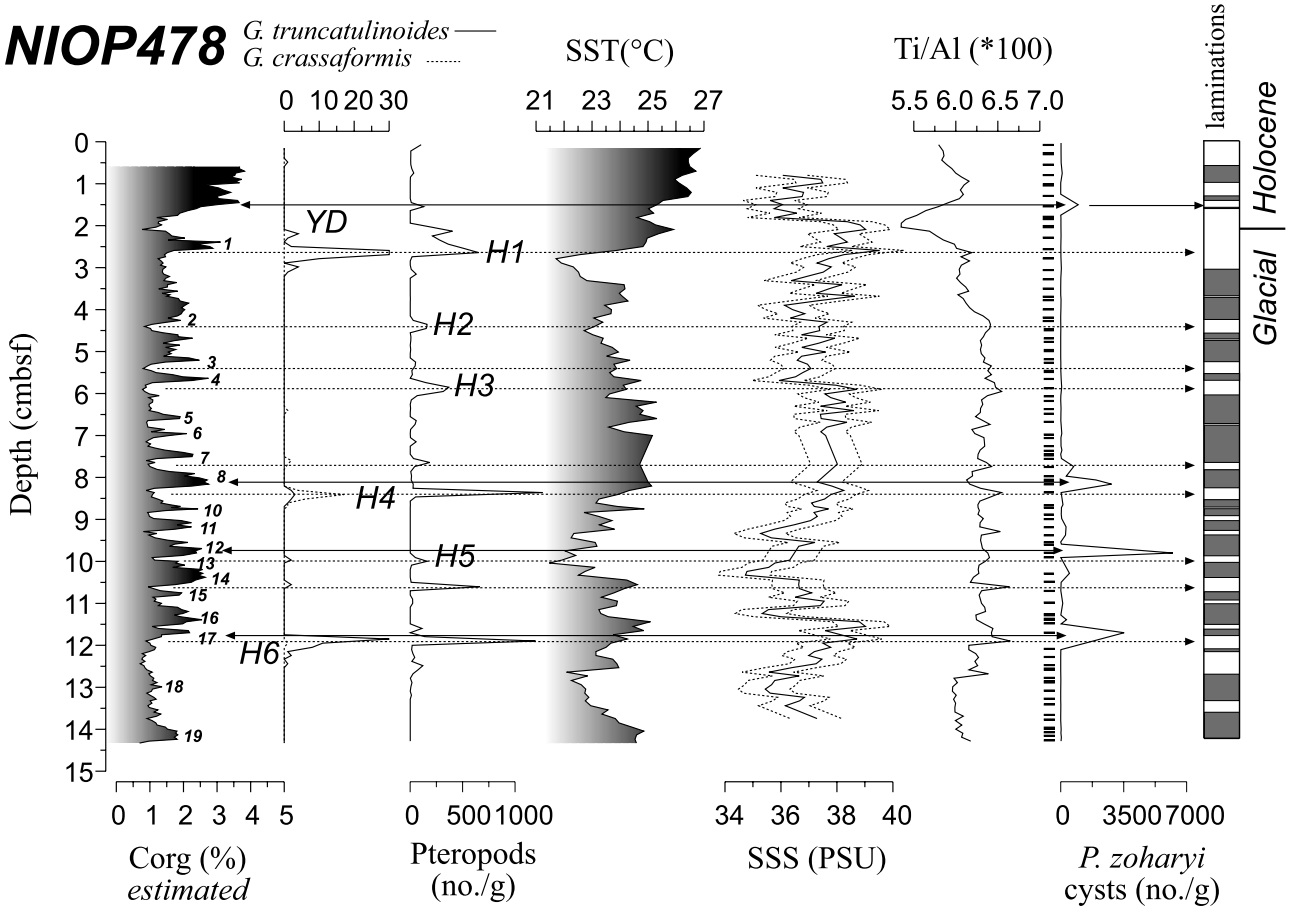

Figure 3. Records of C_{org} (predicted), occurrences of the deep dwelling planktonic foraminifera *G. truncatulinoides* and *G. crassaformis*, pteropod abundance, reconstructed SST and SSS [*Reichart et al.*, 2002b], Ti/Al ratio, and abundance of *P. zoharyi* cysts. On the right side, laminated intervals are indicated in gray. Position of palynological samples is indicated with thin horizontal lines next to *P. zoharyi* record. Numbers 1–19 indicate interstadials as correlated from the GISP2 ice core (Figure 2a). Solid lines with arrows indicate events characterized by *P. zoharyi*; dashed lines with arrows indicate events characterized by proxies for bottom water oxgenation. H1–H6 refer to Heinrich events 1–6; YD refers to the Younger Dryas.

The Sr-rich phase is present only at higher Ca concentrations, which (if both Ca and Sr are present dominantly in two phases) has a Sr/Ca ratio of 0.037–0.007 = 0.03 (Figure 2c).

[11] Maximum Sr/Ca ratios are measured at levels with high numbers of pteropods (2A). This suggests that the Sr-rich Ca phase is somehow related to pteropods (Figures 2a and 2c) since their tests are made out of aragonite, which potentially can have higher Sr concentrations than calcite [*Kinsman and Holland*, 1969]. Sr measurements on pteropod tests from tow samples, however, show concentrations of about 700 ppm (Ulysses S. Ninnemann, University of Bergen, personal communication, 2002). Such low values imply that pteropods cannot explain the excess Sr, which must be incorporated in another sedimentary fraction. The measured Sr/Ca ratios imply that this fraction has an average Sr concentration of 12000 ppm, and thus a partitioning coefficient for Sr of about 1.3. Such a high partitioning coefficient is close to that for inorganic aragonite precipitation, and similar to that of corals [*de Villiers et al.*, 1995]. The close correspondence between high Sr values and well-preserved pteropods also suggests that the Sr-rich fraction is aragonitic. Since aragonite is readily dissolved at the sediment water interface within the OMZ [*Berger*, 1978], the Sr/Ca ratio is an excellent marker for OMZ intensity at site NIOP478. Earlier pteropod and aragonite accumulation events at times of high oxygen conditions remain preserved as increased alkalinities deeper in the sediment due to sulphate reduction prevent the aragonite from dissolving. Sediments deposited during the coldest stadials show high Sr/Ca ratios and are bioturbated, confirming well-oxygenated bottom water conditions. The negative correlation between C_{org} and Sr/Ca during stadials furthermore shows that well-oxygenated bottom waters are associated with minimum surface water productivity conditions and oxygen consumption rates.

[12] Organic-walled dinoflagellate cysts from heterotrophic *Protoperidinium* spp. generally dominate cyst assemblages from NIOP 478. This reflects high-productivity conditions [*Reichart and Brinkhuis*, 2003]. Phototrophic gonyaulacoid

cysts are usually quite rare and are mainly represented by sparse occurrences of oligotrophic *Impagidinium* and cosmopolitan *Spiniferites* cysts. Sudden massive *Polysphaeridium zoharyi* influxes are recorded during warm interstadial events 17, 12 and 8 following Heinrich events H6, H5 and H4, and during the Holocene warming following the Younger Dryas cold phase (Figure 3).

4. Discussion

[13] The well-oxygenated conditions in the northern Arabian Sea during stadials are probably due to convective mixing by intensified and cold winter monsoonal winds [*Reichart et al.*, 1998, 2002b]. Evidence for this comes from the coldest stadials (H1, H4 and H6). These stadials show maximum numbers of the deep dwelling *G. crassaformis* and *G. truncatulinoides*, and pteropods along with high Sr/Ca values, indicating a well-ventilated water column.

[14] All stadials show maxima in Ti/Al ratios, except for the Younger Dryas (YD; Figure 3). The Ti/Al ratio of the sediment is largely controlled by the mineral content. Titanium is known to be concentrated in the coarser sediment fraction, particularly in the heavy mineral assemblage which often contains ilmenite, rutile, titanomagnetite, and augite [*Schmitz*, 1987]. At site NIOP478, these Ti/Al maxima must therefore reflect maximum dust input [*Prins et al.*, 2000]. A satellite image taken during the winter monsoon clearly shows a large dust plume over the northern Arabian Sea leaving the Pakistan coast (Figure 1). During summer, fine-grained fluvial sediments from the Indus River dominate terrigenous supply.

[15] Coarser grained sediments deposited during stadials support our scenario in which intensified winter monsoonal winds drive deep convective overturn, oxygenating bottom waters (shown by higher Sr/Ca values, high numbers of pteropods and bioturbation). Only during the stadials corresponding to Heinrich events H1, H4, possibly H5, and H6 was the depth of convective turnover probably sufficiently deep to support standing stocks of *G. crassaformis* and/or *G. truncatulinoides*. The broad maximum in Ti/Al ratios during deglaciation (including the YD) has a different origin and is most likely due to extra input of fine grained material, possibly through meltwater from the Himalayas via the Indus River.

[16] Glacial alkenone-based SSTs are lower than Holocene values. Minimum SSTs are observed during the stadials corresponding with Heinrich events (Figure 3). Reconstructed SSS values indicate raised salinities during most Heinrich events, which in combination with low SST values would have facilitated deep convective mixing [*Reichart et al.*, 2002b].

[17] Simultaneous changes in the degree of bioturbation, in the Sr/Ca and Ti/Al ratios, in the C_{org} content, and in the numbers of pteropods and deep dwelling planktic foraminifera thus suggest midwater ventilation and low productivity during stadials, whereas midwater dysoxia and eutrophy prevailed during interstadials. Midwater ventilation and reduced upwelling would both contribute to lower C_{org} values during stadials. The pattern exhibited by these rapid changes is similar to the cold-warm switches seen in the Greenland ice cores.

[18] Influxes of *Polysphaeridium zoharyi* cysts immediately following the stadials corresponding to H6, H5, H4, and the YD suggest that these are related to the abrupt warming events following these stadials. Since these transitions are relatively short (<250 years), *P. zoharyi* fluxes must have been large to explain the recorded high numbers of cysts per gram.

[19] *Polysphaeridium zoharyi* represents the cyst stage of *Pyrodinium bahamiense*, a "red tide" species well known from middle to low latitude hyposaline or hypersaline lagoons [e.g., *Wall et al.*, 1977; *Morzadec-Kerfourn*, 1983; *Bradford and Wall*, 1984; *Edwards and Anderle*, 1992; *Lynn Wingard et al.*, 1995]. The life cycle of this euryhaline dinoflagelate species involves the regular formation of nonmotile hypnozygote resting cysts. Vital to the successful germination and regeneration of these cysts is their tolerance to extreme salinities and shallow water depth.

[20] Known to currently dominate surface sediments in the hypersaline shallow Persian Gulf [*Bradford and Wall*, 1984], similar favourable conditions for *P. zoharyi* must have extended into the open Arabian Sea during the transition from cold stadials to warm interstadials. The spikes of *P. zoharyi* in sediments rich in organic matter cannot be explained by large-scale sediment shedding from the continental shelf since these sediments are relatively poor in organic matter. These unusual *P. zoharyi* spikes, therefore, suggest that the northern Arabian Sea experienced conditions unknown in this area today. We hypothesize that a strong and shallow pycnocline following Heinrich events provided a virtual seafloor, enabling *P. zoharyi* to complete its life cycle prior to sinking to deep water.

[21] Recent SSS reconstructions in the northern Arabian Sea have revealed high sea-surface salinities during Heinrich events [*Reichart et al.*, 2002b]. Presently, saline surface waters flow into the Persian Gulf and Red Sea and are returned to the Arabian Sea at depth (Figure 4). A lower sea level at glacial time resulted in a desiccated Persian Gulf and strongly reduced exchange between the Red Sea and the Arabian Sea. Consequently, the excess salt in the surface waters due to ongoing evaporation was no longer exported to depth and thus remained at the surface (Figure 4). Maximum salinities may have been reached during stadials due to strong evaporation related to dry and strong winter monsoonal winds. Cooling this highly saline surface water during winter increased the buoyancy loss of the surface water, resulting in densification and deep convective overturn in the northern Arabian Sea [*Reichart et al.*, 2002b]. Rapid warming in the North Atlantic region immediately following the Heinrich events [*Bond et al.*, 1993; *Dansgaard et al.*, 1993] may have been accompanied by weaker and milder winter monsoonal winds, resulting in a reduced buoyancy loss at the sea surface in the northern Arabian Sea. Evidence for a weakened winter monsoon following Heinrich events comes from low Ti/Al ratios, whereas the interruption of deep mixing in the Arabian Sea is marked by the disappearance of the deep dwelling fora-

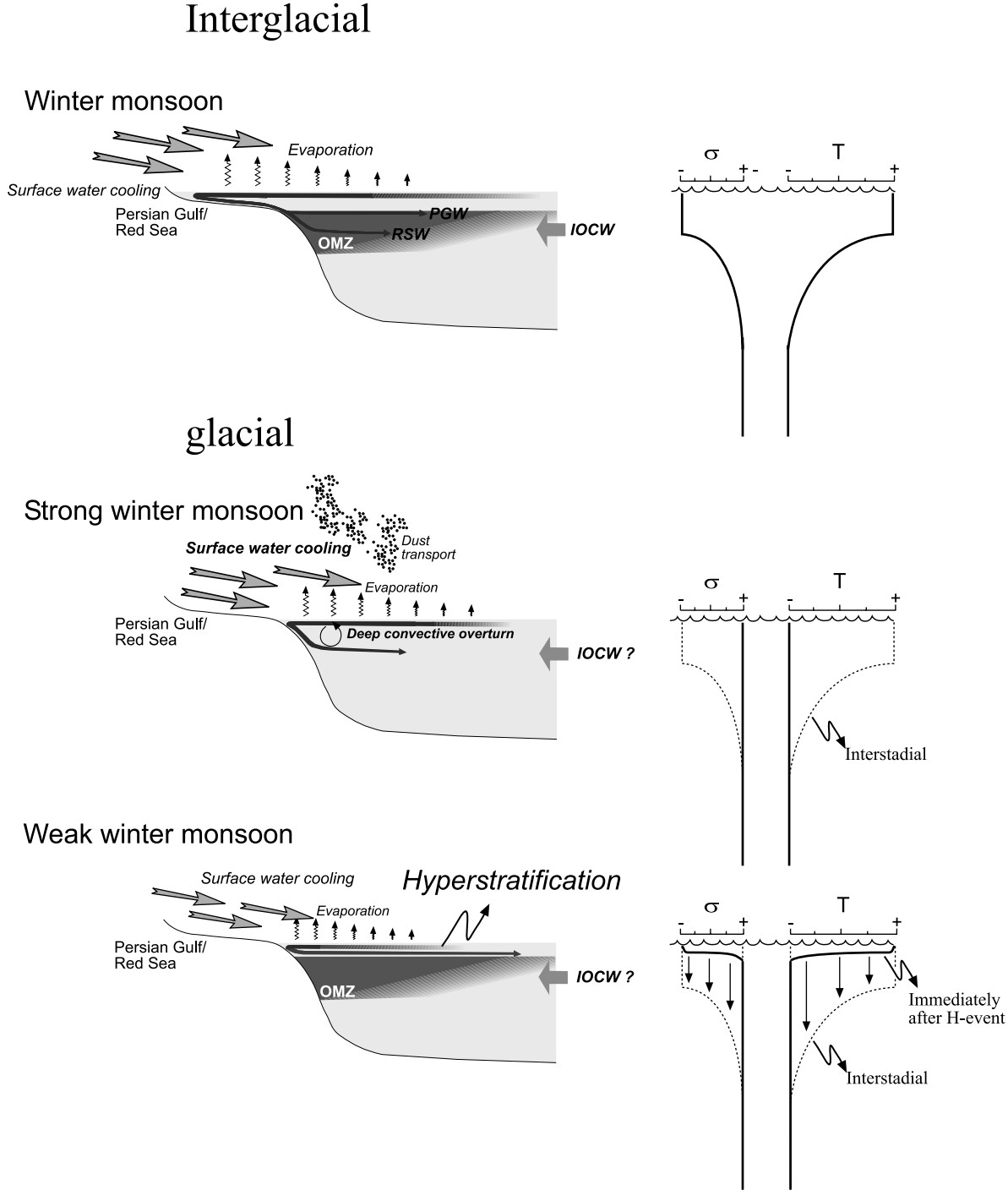

Figure 4. Figures on the left side depict schematic representation of surface and intermediate water circulation during interglacial (present) and glacial times. Schematic graphs on the right give general trends in density (σ) and temperature (T) in the upper part of the water column. Presently, the circulation of the intermediate water is dominated by the inflow of relatively oxygen poor Indian Ocean Central Water (IOCW) and inflow at depth of warm and saline water from the Persian Gulf and Red Sea (upper diagrams). The two glacial scenarios represent full stadial conditions (middle diagram) and the transition from stadial to interstadial (lower diagram). The brief periods of hyperstratification at stadials-interstadial transitions are inferred from the *P. zoharyi* data presented in this study.

miniferal species *G. crassaformis* and *G. truncatulinoides*. If this weakening of the winter monsoon predated the subsequent strengthening of the summer monsoon then a shallow and strong pycnocline could have developed in the northern Arabian Sea during a short period following the Heinrich events (Figure 4). This phenomenon, here referred to as "hyperstratification," in combination with high stadial SSS values, would have provided optimum habitat conditions for *P. zoharyi*. Erosion of this shallow pycnocline by wind-driven mixing related to intense (early) summer monsoonal winds during full interstadials should have resulted in a deeper annual mixed layer (Figure 4).

[22] The warmings following the stadials corresponding to Heinrich events 1, 2 and 3 apparently lack *P. zoharyi* spikes. It is clear that sea-surface conditions following Heinrich event 1 were different from those following all other Heinrich events since prolonged deep mixing seems to have continued nearly into the Holocene. Evidence for this comes from the continued presence of pteropods and *G. truncatulinoides*, whereas sediments remain clearly bioturbated (Figure 3). The reason why *P. zoharyi* spikes are missing after Heinrich events 3 and 2 is, however, less evident. In view of the sample resolution used (Figure 3) it seems unlikely that we missed a *P. zoharyi* spike corresponding to those intervals, although it can not be excluded that these *P. zoharyi* blooms were extremely short-lived events. More likely, hyperstratification may develop under only a narrow range of boundary conditions. Reduced regional warming, caused by overall increased glacial conditions at those times [*Cutler et al.*, 2003; *Mix et al.*, 2001; *Weaver et al.*, 1999], may have prevented development of the shallow density gradient needed for *P. zoharyi* to bloom. Conditions comparable to those following Heinrich events 6, 5, and 4 again prevailed for the transition from the Younger Dryas to the Holocene climatic optimum (Figure 3).

[23] A relatively stable OMZ re-established itself at the beginning of the Holocene with the OMZ, just as today, being ventilated from the south by Indian Ocean Central Waters with minor contributions from Persian Gulf and Red Seawaters.

5. Conclusions

[24] Arabian Sea hydrography during the last glacial shows a series of rapid switches coinciding with the Dansgaard-Oeschger climatic changes, interstadials being characterized by an intense OMZ, while stadials show a well-ventilated water column. During the coldest stadials deep convective mixing locally ventilated the subsurface water. New dinoflagellate data presented here shows abrupt influxes of *P. zoharyi* cysts immediately following several periods (H6-4, YD) characterized by deep mixing. These *P. zoharyi* cyst spikes suggest the occurrence of brief episodes of hyperstratification in the Northern Arabian Sea. This phenomenon might have been instrumental in the rapid re-establishment of an OMZ during the onset of interstadials as inferred from nitrogen isotopes [*Altabet et al.*, 2002].

[25] **Acknowledgments.** F. Ammerlaan and D. van der Akker are kindly thanked for assisting with data generation. J. van Tongeren and N. Welters are thanked for the palynological processing. G. Nobbe, A. van Dijk, G. Ittman and G. van het Veld are acknowledged for laboratory assistance. We thank Karin Zonneveld and Jörg Pross for their constructive reviews.

References

Altabet, M. A., R. Francois, D. W. Murray, and W. L. Prell (1995), Climate-related variations in denitrification in the Arabian Sea from sediment N-15/N-14 ratios, *Nature*, *373*, 506–509.

Altabet, M. A., M. J. Higginson, and D. W. Murray (2002), The effect of millennial-scale changes in Arabian Sea denitrification on atmospheric CO2, *Nature*, *415*, 159–162.

Berger, W. H. (1978), Deep-sea carbonate: Pteropod distribution and the aragonite compensation depth, *Deep Sea Res. Part I*, *25*, 447–452.

Bond, G., W. Broecker, S. Johnsen, J. McManus, L. Labeyrie, J. Jouzel, and G. Bonani (1993), Correlations between climate records from North-Atlantic sediments and Greenland ice, *Nature*, *365*(6442), 143–147.

Bradford, M. R., and D. A. Wall (1984), The distribution of recent organic-walled dinoflagellate cysts in the Persian Gulf, Gulf of Oman, and northwestern Arabian Sea, *Palaeontographica, Ser. B*, *192*, 16–84.

Cutler, K. B., R. L. Edwards, F. W. Taylor, H. Cheng, J. Adkins, C. D. Gallup, P. M. Cutler, G. S. Burr, and A. L. Bloom (2003), Rapid sea-level fall and deep-ocean temperature change since the last interglacial period, *Earth Planet. Sci. Lett.*, *206*, 253–271.

Dansgaard, W., et al. (1993), Evidence for general instability of past climate from a 250-Kyr ice-core record, *Nature*, *364*, 218–220.

de Villiers, S., B. K. Nelson, and A. R. Chivas (1995), Biological controls on coral Sr/Ca and $\delta^{18}O$ reconstructions of sea surface temperatures, *Science*, *269*, 1247–1249.

Edwards, L. E., and V. Anderle (1992), Distribution of selected dinoflagellate cysts in modern marine sediments, in *Neogene and Quaternary Dinoflagellate Cysts and Acritharchs*, edited by M. J. Head and J. H. Wrenn, pp. 259–273, Am. Assoc. of Stratigr. Palynol., Houston, Tex.

Grootes, P. M., M. Stuiver, J. W. C. White, S. Johnsen, and J. Jouzel (1993), Comparison of oxygen-isotope records from the Gisp2 and Grip Greenland ice cores, *Nature*, *366*, 552–554.

Jannink, N. T., W. J. Zachariasse, and G. J. Van der Zwaan (1998), Living (Rose Bengal stained) benthic foraminifera from the Pakistan continental margin (northern Arabian Sea), *Deep Sea Res. Part I*, *45*, 1483–1513.

Kinsman, D. J. J., and H. D. Holland (1969), The co-precipitation of cations with CaCO3—IV. The co-precipitation of Sr2+ with aragonite between 16°C and 96°C, *Geochim. Cosmochim. Acta*, *33*, 1–17.

Lynn Wingard, G., S. Ishman, T. Cronin, L. E. Edwards, D. A. Willard, and R. B. Halley (1995), Preliminary analysis of down-core biotic assemblages: Bob Allen Keys, Everglades National Park, Florida Bay, *Rep. OFR-95-628*, U.S. Geol. Surv., Reston, Va.

Mix, A. C., E. Bard, and R. Schneider (2001), Environmental processes of the ice age: Land, oceans, glaciers (EPILOG), *Quat. Sci. Rev.*, *20*, 627–657.

Morzadec-Kerfourn, M.-T. (1983), Intérêt des kystes de dinoflagellés pour l'établishment of reconsititution paléogéographique: Example du Golf de Gablès (Tunisie), *Cah. Micropaleontol.*, *4*, 15–22.

Naqvi, S. W. A. (1987), Some aspects of the oxygen deficient conditions and denitrification in the Arabian Sea, *J. Mar. Res.*, *45*, 1049–1072.

Olson, D. B., G. L. Hitchcock, R. A. Fine, and B. A. Warren (1993), Maintenance of the low-oxygen layer in the central Arabian Sea, *Deep Sea Res. Part II*, *40*, 673–685.

Prins, M. A., G. Postma, J. Cleveringa, A. Cramp, and N. H. Kenyon (2000), Controls on terrigenous sediment supply to the Arabian Sea during the late Quaternary: The Indus Fan, *Mar. Geol.*, *169*, 327–349.

Reichart, G. J., and H. Brinkhuis (2003), Late Quaternary *Protoperidinium* cysts as indicators of paleoproductivity in the northern Arabian Sea, *Mar. Micropaleontol.*, *49*, 303–315.

Reichart, G. J., L. J. Lourens, and W. J. Zachariasse (1998), Temporal variability in the northern Arabian Sea Oxygen Minimum Zone (OMZ) during the last 225,000 years, *Paleoceanography*, *13*, 607–621.

Reichart, G. J., S. J. Schenau, G. J. de Lange, and W. J. Zachariasse (2002a), Synchroneity of oxygen minimum zone intensity on the Oman

and Pakistan Margins at sub-Milankovitch time scales, *Mar. Geol.*, *185*, 403–415.

Reichart, G. J., J. Nortier, G. J. M. Versteegh, and W. J. Zachariasse (2002b), Periodical breakdown of the Arabian Sea oxygen minimum zone caused by deep convective mixing, in *The Tectonic and Climatic Evolution of the Arabian Sea Region*, edited by P. D. Clift et al., pp. 407–420, Geol. Soc., London.

Schmitz, B. (1987), The TiO_2/Al_2O_3 ratio in the Cenozoic Bengal abyssal fan sediments and its use as a paleostream energy indicator, *Mar. Geol.*, *76*, 195–206.

Schulz, H., U. von Rad, and H. Erlenkeuser (1998), Correlation between Arabian Sea and Greenland climate oscillations of the past 110,000 years, *Nature*, *393*, 54–57.

Schulz, H., K.-C. Emeis, H. Erlenkeuser, U. von Rad, and C. Rolf (2002), The Toba volcanic event and interstadial/stadial climates at the marine isotopic stage 5 to 4 transition in the northern Indian Ocean, *Quat. Res.*, *57*, 22–31.

Swallow, J. C. (1984), Some aspects of the physical oceanography of the Indian Ocean, *Deep Sea Res. Part I*, *31*, 639–650.

van der Weijden, C. H., G. J. Reichart, and H. J. Visser (1999), Enhanced preservation of organic matter in sediments deposited within the oxygen minimum zone in the northeastern Arabian Sea, *Deep Sea Res. Part I*, *46*, 807–830.

Von Stackelberg, U. (1972), Faziesverteilung in Sedimenten des Indisch-Pakistanischen Kontinentalrandes (Arabisches Meer), *Meteor Forschungs. Reihe C*, 1–73.

Wall, D. A., B. Dale, G. P. Lohmann, and W. Smith (1977), The environmental and climatic distribution of dinoflagellate cysts in modern marine sediments from regions in the North and South Atlantic Oceans and adjacent seas, *Mar. Micropaleontol.*, *2*, 121–144.

Weaver, P. P. E., M. R. Chapman, G. Eglinton, M. Zhao, D. Rutledge, and G. Read (1999), Combined coccolith, foraminiferal, and biomarker reconstruction of paleoceanographic conditions over the past 120 kyr in the northern North Atlantic (59°N, 13°W), *Paleoceanography*, *14*, 336–349.

Williams, G. L., J. K. Lentin, and R. A. Fensome (1998), *The Lentin and Williams Index of Fossil Dinoflagellates*, 817 pp., Am. Assoc. of Stratigr. Palynol., Houston, Tex.

Wyrtki, K. (1971), *Oceanographic Atlas of the International Indian Ocean Expedition*, 531 pp., Natl. Sci. Found., Arlington, Va.

Wyrtki, K. (1973), Physical oceanography of the Indian Ocean, in *The Biology of the Indian Ocean*, edited by B. Zeitschel, pp. 18–36, Springer-Verlag, New York.

You, Y., and M. Tomczak (1993), Thermocline circulation and ventilation in the Indian Ocean derived from water mass analysis, *Deep Sea Res. Part I*, *40*, 13–56.

H. Brinkhuis, Laboratory of Palaeobotany and Palynology, Utrecht University, Budapestlaan 4, 3584 CD Utrecht, Netherlands.

F. Huiskamp and W. J. Zachariasse, Faculty of Earth Sciences, Utrecht University, Budapestlaan 4, 3584 CD Utrecht, Netherlands.

G.-J. Reichart, Alfred Wegener Institut for Polar and Marine Research, Am Handelshafen 12, Building Co-12, D-27570 Bremerhaven, Germany. (greichart@awi-bremerhaven.de)